The Energy and Angular Momentum Budgets of a Three-Dimensional Tropical Cyclone Model

ROBERT E. TULEYA AND YOSHIO KURIHARA

Geophysical Fluid Dynamics Laboratory/NOAA, Princeton University, Princeton, N. J. 08540

(Manuscript received 15 March 1974, in revised form 9 September 1974)

ABSTRACT

Energy and angular momentum budgets are analyzed for a three-dimensional model hurricane described by Kurihara and Tuleya.

Eddies which developed in the model are maintained in the mature stage by energy supply from both mean kinetic and total potential energy. In the evolution of eddies during the early development stage of the storm, the supply from potential energy is more important.

Eddies export latent, internal, kinetic energy and relative angular momentum from the storm core region. They also contribute to the outward transfer of energy through pressure work. However, the mean flow dominates the transport by importing those quantities into the inner area and exporting potential energy.

The energy and angular momentum budgets are primarily controlled by the mean flow, though the role of eddies is not negligible for the budgets of angular momentum, kinetic and latent energy in the inner region. For the maintenance of mean kinetic energy in the inner area, both generation and advection make positive contributions.

The computed transports and budgets are compared with those available for other three-dimensional models as well as with real data analyses made by other investigators.

1. Introduction

Numerical simulation models of tropical cyclones have been developed and analyzed at the Geophysical Fluid Dynamics Laboratory/NOAA. Both axisymmetric and three-dimensional models have been successfully integrated and the basic results of a three-dimensional model integration were published by Kurihara and Tuleya (1974). This model successfully simulated a hurricane-like structure including a warm moist core, low level inflow, and spiral bands.

A brief review of the three-dimensional numerical model and some results of the integration are given in Section 2. Although the present model was constructed with some simplifying conditions and constraints which have to be removed in the future, it is still informative to make an analysis of a model in which asymmetries have evolved from an initially circular vortex. This paper discusses in detail the energy and angular momentum budgets of the model. The total energy of the model may be partitioned into the kinetic energy of the mean flow, the kinetic energy of eddy motion, the total potential (potential plus internal) energy, and the latent energy. The budget of each form of energy is analyzed in Section 3. The analysis of eddy kinetic energy reveals the energy conversion processes which are responsible for the development and maintenance of eddy motion. In this section an attempt is also made to relate the band structure of the model to eddy transports of specific quantities. In Section 4 the analysis of the angular momentum budget is presented. In discussing the budgets of the above quantities, the role of eddy asymmetries and their contribution relative to the mean flow are emphasized. The results are summarized in Section 5.

Some previous budget studies of tropical cyclones based on real data are those, for example, by Palmén and Riehl (1957), Malkus and Riehl (1960), Riehl and Malkus (1961), Hawkins and Rubsam (1968) and Black and Anthes (1971). Some information was obtained in these analyses about the asymmetrical structure of tropical cyclones and its role in the budgets of energy and angular momentum. In case of real data analyses, the asymmetry which is associated with the movement of hurricanes may also contribute to a significant degree to the eddy transport of quantities. Such an asymmetry related to a basic flow does not exist in the present model. This difference must be remembered when the eddy transports in the model are compared with observational estimates.

Anthes (1972) analyzed some of the budget terms of a three-dimensional model hurricane and Mathur (1972) has computed the angular momentum transport of a simulation experiment. Some of the results from the above-mentioned studies will be compared with the GFDL model's results.

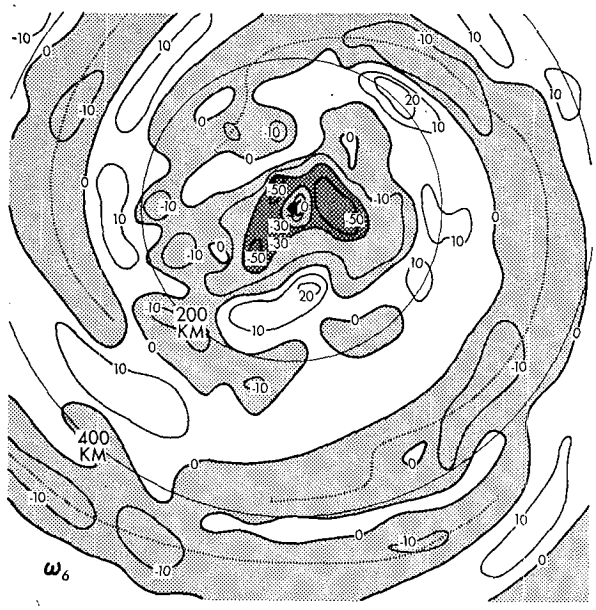

FIG. 1. Distribution of ω ($=dp/dt$) at level 6 at Hour 151 of the model integration. Area of negative ω is shaded. Center of bands are indicated by dotted lines. Units are 10^{-3} mb s^{-1}.

2. Brief review of model

As mentioned in the Introduction, the model used for the budget analyses is the one presented by Kurihara and Tuleya (1974). The three-dimensional, eleven-level primitive equation model has four levels in the boundary layer and its 70×70 variable grid mesh encloses a 4000 km square domain. The grid resolution near the center is 20 km. Parameterization schemes for convective processes and subgrid-scale diffusion are included. The Coriolis parameter f is 5×10^{-5} s^{-1} throughout the domain.

The model hurricane develops from a weak, balanced vortex which is given as the initial state. Typical of the tropics during hurricane season, the model atmosphere is conditionally unstable at the beginning and the sea surface temperature is set at 302 K for the entire integration.

After three days of integration, hurricane force winds are present in the lowest layer of the model and the central surface pressure drops below 970 mb. By 6 days, the interior of the storm is in a quasi-steady state with winds at the lowest level on the order of 50 m s^{-1} and a central surface pressure about 945 mb. Heavy precipitation patterns are evident throughout the development and mature stages of the model storm. The model is successful in the development and maintenance of shallow, low-level inflow, asymmetric upper-level outflow, and a warm, moist core typical of tropical cyclones. Spiral bands also develop and move radially outward. Most of the precipitation in the outer regions of the storm falls within the bands. An area having the eye-like features of subsidence and relatively light precipitation is often found near the area of lowest pressure.

The asymmetries developed in the model appear not to be random perturbations. As an example, the distributions of the vertical pressure velocity ω at the sixth level of the model, ~3300 m above the surface, at Hour 151 of the integration, is shown in Fig. 1. In this field the asymmetries take the form of spiral bands in the outer region of the storm and two to three cells of upward motion surrounding the eye in the interior. In the case of the outflow field in the upper troposphere, the asymmetries are not randomly distributed but organized in a pattern of several narrow streams extending outward from the storm core area (Fig. 12 in Kurihara and Tuleya, 1974). The organized asymmetries as mentioned above are probably the dominant components of eddies to be defined in the following sections.

3. Energy budget

a. Energy equations

1) KINETIC ENERGY

The kinetic energy was divided into an azimuthal mean part, referred to as mean kinetic energy K_M and the difference between the total and mean kinetic energy, referred to as eddy kinetic energy K_E. To derive the equations for kinetic energy, one starts with the two horizontal components of the equation of motion and the continuity equation written in cylindrical coordinates with sigma coordinates used in the vertical (Phillips, 1957):

$$\frac{\partial}{\partial t}(p_* v_r) = -D(v_r) + (f + v_\theta/r) p_* v_\theta - p_* \frac{\partial \phi_p}{\partial r} + F_r, \quad (3.1)$$

$$\frac{\partial}{\partial t}(p_* v_\theta) = -D(v_\theta) - (f + v_\theta/r) p_* v_r - p_* \frac{\partial \phi_p}{r \partial \theta} + F_\theta, \quad (3.2)$$

$$\frac{\partial}{\partial t}(p_*) = -D(1), \quad (3.3)$$

where t is the time, r the radius, v_r and v_θ the radial and tangential velocity components, and p_* the surface pressure. The operator D denotes the three-dimensional divergence:

$$D(\ ) = \frac{\partial(\ ) p_* r v_r}{r \partial r} + \frac{\partial(\ ) p_* v_\theta}{r \partial \theta} + \frac{\partial(\ ) p_* \dot{\sigma}}{\partial \sigma}, \quad (3.4)$$

where $\sigma = p/p_*$, p is the pressure, and $\dot{\sigma}$ the vertical σ-velocity, i.e., $d\sigma/dt$. The pressure gradient force is estimated from the gradient of ϕ_p, the geopotential on a constant pressure surface. The last term in (3.1) and (3.2) represents the horizontal and vertical diffusion of momentum. Further information of the details of the model formulation is contained in the paper by Kurihara and Tuleya (1974).

Multiplying (3.1) by v_r and (3.2) by v_θ and using the continuity equation (3.3), one obtains the equation for total kinetic energy. To separate the kinetic energy into eddy and mean components one defines:

$$\left.\begin{aligned} v_r &= \bar{v}_r + v_r' \\ v_\theta &= \bar{v}_\theta + v_\theta' \end{aligned}\right\}, \tag{3.5}$$

where a bar refers to an azimuthal average or mean and a prime is the deviation from the mean.

The mean and eddy components of other quantities may be defined by expressions similar to (3.5). The mean flow and the eddies thus defined naturally depend on the choice of a reference surface on which the average is taken. In the present analyses, the mean and eddy components are computed at a constant σ level. However, they can be thought to apply on a constant height level because the undulation of a σ surface is very small in the azimuthal direction. This is because surface pressure and temperature are almost axisymmetric.

By substituting (3.5) into the expression for total kinetic energy and by taking the azimuthal average, the tendency of total kinetic energy for a ring is obtained in terms of averages and deviations from the mean. The kinetic energy equation for the mean flow is obtained by using (3.5) in the basic equations (3.1) and (3.2), taking the azimuthal average, and then multiplying by the azimuthal mean velocities $\bar{v}_r$ and $\bar{v}_\theta$. By subtracting the equation for the mean kinetic energy from the total kinetic energy, the eddy kinetic energy equation is obtained. In this analysis the origin of the cylindrical coordinates is placed at the surface pressure minimum. The variation of p_* along a radius circle is very small. Therefore, for the simplification of analysis, p_* is assumed to be a function of radius and time only, i.e., $p_*=\bar{p}_*(r,t)$. Actually, the standard deviation of p_* in the azimuthal direction is generally less than a millibar at any radius throughout the integration period of the model.

One can express the mean and eddy kinetic energy equations in a vertically integrated form as

$$\begin{aligned} \frac{\partial}{\partial t}\{K_M\} = & && \text{tendency of } K_M \\ & -\frac{\partial}{r\partial r}(r\{\mathrm{FLXM}\}) && \text{flux convergence of } K_M \\ & -\{K_M,K_E\} && \text{conversion between } K_M \text{ and } K_E \\ & +\{TP,K_M\} && \text{generation of } K_M \text{ from total potential energy} \\ & +\{K_M,\mathrm{Diss}\} && \text{dissipation of } K_M \end{aligned} \tag{3.6}$$

$$\begin{aligned} \frac{\partial}{\partial t}\{K_E\} = & && \text{tendency of } K_E \\ & -\frac{\partial}{r\partial r}(r\{\mathrm{FLXE}\}) && \text{flux convergence of } K_E \\ & +\{K_M,K_E\} && \\ & +\{TP,K_E\} && \text{generation of } K_E \text{ from total potential energy} \\ & +\{K_E,\mathrm{Diss}\} && \text{dissipation of } K_E \end{aligned} \tag{3.7}$$

where TP refers to the total potential energy, Diss the frictional dissipation, and $\{\ \}$ denotes the azimuthal average of a vertically integrated quantity. If we define

$$\langle(\ )\rangle \equiv \int_0^1 (\ )\,d\sigma/g,$$

then

$$\{K_M\} = \left\langle p_*\left(\frac{\bar{v}_r^2+\bar{v}_\theta^2}{2}\right)\right\rangle$$

$$\{K_E\} = \left\langle p_*\left(\frac{\overline{v_r'^2}+\overline{v_\theta'^2}}{2}\right)\right\rangle$$

$$\{\mathrm{FLXM}\} = \left\langle p_*\bar{v}_r\left(\frac{\bar{v}_r^2+\bar{v}_\theta^2}{2}\right)\right\rangle$$

$$\{\mathrm{FLXE}\} = \{\mathrm{FLXE}\}_M + \{\mathrm{FLXE}\}_E$$

$$\{\mathrm{FLXE}\}_M = \left\langle p_*\bar{v}_r\left(\frac{\overline{v_r'^2}+\overline{v_\theta'^2}}{2}\right)\right\rangle$$

$$\{\text{FLXE}\}_E=\left\langle p_*\bar{v}_r\overline{v_r'v_r'}+p_*\bar{v}_\theta\overline{v_r'v_\theta'}+p_*\overline{v_r'\frac{v_r'^2+v_\theta'^2}{2}}\right\rangle$$

$$\{K_M,K_E\}=\{K_M,K_E\}_H+\{K_M,K_E\}_V$$

$$\{K_M,K_E\}_H=\left\langle \bar{v}_r\frac{\partial}{r\partial r}(p_*\overline{rv_r'v_r'})+\bar{v}_\theta\frac{\partial}{r\partial r}(p_*\overline{rv_r'v_\theta'})-\frac{p_*}{r}\bar{v}_r\overline{v_\theta'v_\theta'}+\frac{p_*}{r}\bar{v}_\theta\overline{v_\theta'v_r'}\right\rangle$$

$$\{K_M,K_E\}_V=\left\langle \bar{v}_r\frac{\partial}{\partial\sigma}(p_*\overline{v_r'\dot{\sigma}'})+\bar{v}_\theta\frac{\partial}{\partial\sigma}(p_*\overline{v_\theta'\dot{\sigma}'})\right\rangle$$

$$\{TP,K_M\}=\left\langle -p_*\bar{v}_r\frac{\partial\bar{\phi}_p}{\partial r}\right\rangle$$

$$\{TP,K_E\}=\left\langle -p_*\overline{v_r'\frac{\partial\phi_p'}{\partial r}}-p_*\overline{v_\theta'\frac{1}{r}\frac{\partial\phi_p'}{\partial\theta}}\right\rangle$$

$$\{K_M,\text{Diss}\}=\{K_M,\text{Diss}\}_H+\{K_M,\text{Diss}\}_V$$

$$\{K_M,\text{Diss}\}_H=\langle\bar{v}_{r\,H}\bar{F}_r+\bar{v}_{\theta\,H}\bar{F}_\theta\rangle$$

$$\{K_M,\text{Diss}\}_V=\langle\bar{v}_{r\,V}\bar{F}_r+\bar{v}_{\theta\,V}\bar{F}_\theta\rangle$$

$$\{K_E,\text{Diss}\}=\{K_E,\text{Diss}\}_H+\{K_E,\text{Diss}\}_V$$

$$\{K_E,\text{Diss}\}_H=\langle\overline{v_r'{}_HF_r'}+\overline{v_\theta'{}_HF_\theta'}\rangle$$

$$\{K_E,\text{Diss}\}_V=\langle\overline{v_r'{}_VF_r'}+\overline{v_\theta'{}_VF_\theta'}\rangle.$$

The term $\{K_M,K_E\}$ appears with different signs in the equations for $\{K_M\}$ and $\{K_E\}$, and represents the conversion of kinetic energy of axisymmetric flow to that of eddy motion. It is due to the eddy flux of momentum. The term $\{TP,K_E\}$ in the equation for $\{K_E\}$ has a counterpart in the equation for total potential energy [(3.8)]. The release of total potential energy through eddy processes is made by the overturning process, i.e., the ascending of relatively warm air and the descending of relatively cold air along a circle of constant radius. The released energy, after being distributed radially through pressure work, eventually becomes a source of $\{K_E\}$. The term $\{TP,K_E\}$ represents the generation of $\{K_E\}$ by the above process. Note that the frictional terms F_r and F_θ of (3.1) and (3.2) have been separated into horizontal and vertical components. In the eddy kinetic energy equation, the first two terms of $\{\text{FLXE}\}_E$ represent the eddy transport of $\bar{v}_\theta v_\theta'$ and $\bar{v}_r v_r'$ which are the locally non-vanishing components of the eddy kinetic energy. In the analysis by Anthes (1972), the contribution from these two terms were included in his definition of energy conversion by horizontal barotropic processes.

2) Total potential energy

The equation for total potential energy, the sum of internal and potential energy ($c_vT+\phi$), can be derived from the first law of thermodynamics. An expression for the tendency of total potential energy TP of an air column in hydrostatic balance is

$$\begin{aligned}
\frac{\partial}{\partial t}\{TP\}= &\quad \text{tendency of } TP\\
-\frac{\partial}{r\partial r}(r\{\text{FLXI}\}) &\quad \text{flux convergence of internal energy}\\
-\frac{\partial}{r\partial r}(r\{\text{FLXP}\}) &\quad \text{flux convergence of potential energy}\\
-\frac{\partial}{r\partial r}(r\{\text{PW}\}) &\quad \text{flux convergence of pressure work}\\
-\{TP,K\} &\quad \text{loss due to generation of kinetic energy}\\
+\{TP,\text{HDIF}\} &\quad \text{horizontal diffusion of } TP\\
+\{TP,\text{VDIF}\} &\quad \text{vertical diffusion of } TP \text{ (surface heat flux)}\\
+\{L,TP\} &\quad \text{gain due to release of latent energy}
\end{aligned}\tag{3.8}$$

where

$$\{TP\} = \langle p_*(c_v\bar{T}+\bar{\phi})\rangle = \langle p_* c_p \bar{T}\rangle$$

$$\{\text{FLXI}\} = \{\text{FLXI}\}_M + \{\text{FLXI}\}_E$$

$$\{\text{FLXI}\}_M = \langle p_* \bar{v}_r c_v \bar{T}\rangle$$

$$\{\text{FLXI}\}_E = \langle p_* c_v \overline{v_r' T'}\rangle$$

$$\{\text{FLXP}\} = \langle p_* \overline{v_r \phi}\rangle$$

$$\{\text{PW}\} = \{\text{PW}\}_M + \{\text{PW}\}_E$$

$$\{\text{PW}\}_M = \{\text{FLXI}\}_M (R_g/c_v)$$

$$\{\text{PW}\}_E = \{\text{FLXI}\}_E (R_g/c_v)$$

$$\{TP,\text{HDIF}\} = \langle c_{p\,H}\bar{F}_T\rangle$$

$$\{TP,\text{VDIF}\} = \langle c_{p\,V}\bar{F}_T\rangle$$

$$\{L,TP\} = \langle c_p \overline{\text{TADJ}}\rangle.$$

In the above expressions, c_v and c_p are the specific heats at constant volume and pressure, respectively; T is the temperature; ${}_HF_T$ is the horizontal convergence of the diffusive heat flux; ${}_VF_T$ is the vertical convergence of the diffusive heat flux [i.e., $\langle c_{p\,V}F_T\rangle$ is the surface heat flux]; TADJ is the temperature change caused by condensation and convection processes; and R_g is the specific gas constant of air.

3) Latent energy

The expression for the vertical integral of latent energy can be written as

$$\frac{\partial}{\partial t}\{LR\} = \quad \text{tendency of latent energy, } LR$$

$$-\frac{\partial}{r\partial r}(r\{\text{FLXL}\}) \quad \text{flux convergence of latent heat}$$

$$+\{L,\text{HDIF}\} \quad \text{horizontal diffusion of latent energy}$$

$$+\{L,\text{VDIF}\} \quad \text{vertical diffusion of } L \text{ (evaporation)}$$

$$-\{L,TP\} \quad \text{loss of latent energy through condensation} \qquad (3.9)$$

where

$$\{LR\} = \langle p_* L\bar{R}\rangle$$

$$\{\text{FLXL}\} = \{\text{FLXL}\}_M + \{\text{FLXL}\}_E$$

$$\{\text{FLXL}\}_M = \langle p_* L\bar{v}_r\bar{R}\rangle$$

$$\{\text{FLXL}\}_E = \langle p_* L\overline{v_r'R'}\rangle$$

$$\{L,\text{HDIF}\} = \langle L_{\,H}\bar{F}_R\rangle$$

$$\{L,\text{VDIF}\} = \langle L_{\,V}\bar{F}_R\rangle.$$

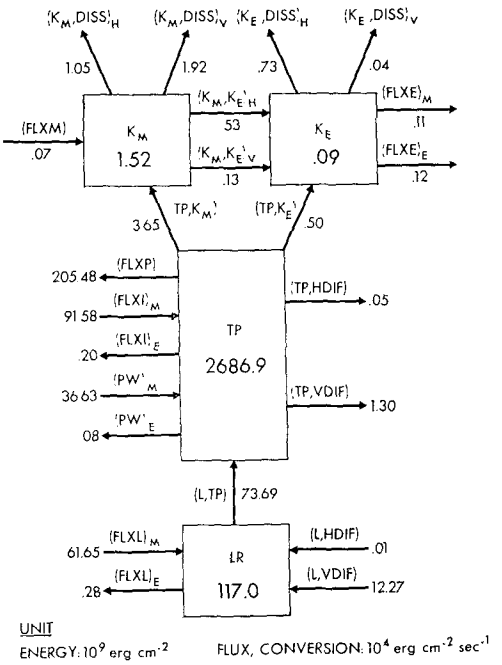

FIG. 2. Energy budget for inner 498 km of the model hurricane averaged for Hours 150–159. The area averages of flux convergences and conversions are in units of 10^4 erg cm^{-2} s^{-1}. The area average energy levels, given within each box, are in units of 10^9 erg cm^{-2}. Energy symbols used are K_M or M (mean kinetic), K_E or E (eddy kinetic), TP (total potential), P (potential), I (internal) and LR or L (latent energy). Notations $(\text{FLX}\alpha)_M$, $(\text{FLX}\alpha)_E$ denote flux convergences of energy α by mean flow and eddies, respectively; (α, HDIF), (α, VDIF) flux convergences of α by horizontal and vertical diffusion, respectively; (α, DISS)$_H$, (α, DISS)$_V$, dissipation of α due to horizontal and vertical stress, respectively; (PW) pressure work. Arrows indicate direction of flux or energy conversion.

In these expressions, R is the mixing ratio; L is the latent heat of condensation; ${}_HF_R$ is the horizontal diffusive flux convergence of mixing ratio; and ${}_VF_R$ is the vertical diffusive flux convergence of mixing ratio [i.e., $\langle {}_VF_R\rangle$ is the evaporation].

In the present study, most of the energy budget analysis is made in a vertically integrated form in order to simplify the analysis and to describe the gross features of the energy balance. The vertical variation of each term in the energy budget equations may be

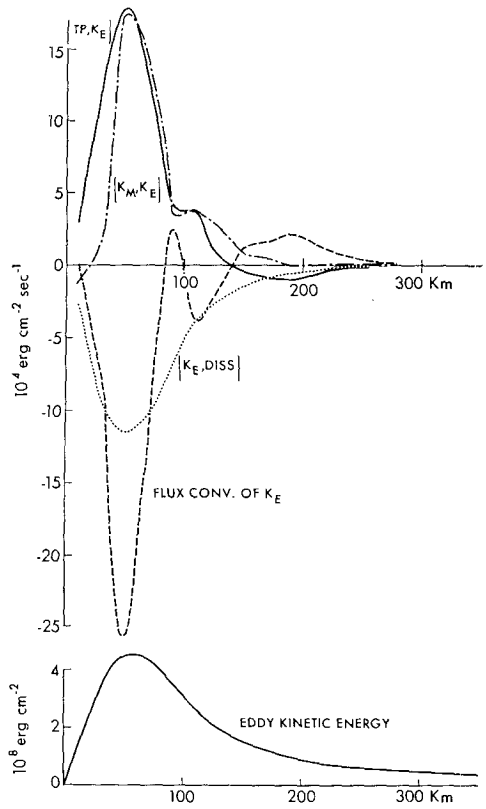

FIG. 3. Radial distribution of eddy kinetic energy and eddy kinetic energy budget for mature storm period (Hours 150–159). Values are vertically integrated, area averages. Changes due to flux convergence (dashed line), conversion from K_M (dash-dotted line), conversion from TP (thick solid line), and dissipation (dotted line) are shown.

analyzed in future work when the generation of eddies will be investigated. A more complete analysis of the vertical variation of various terms in the energy budget was done by Kurihara (1975) for the symmetric analog of the three-dimensional model hurricane analyzed here.

b. Eddy kinetic energy budget

By averaging over several radial intervals, one can obtain a budget description of the energy over the interior of the storm region. Fig. 2 is a box diagram of the model hurricane energy budget averaged from Hours 150 to 159 for the inner 498 km. This is at the mature stage of the model hurricane when the inner storm region is quasi-steady (Kurihara and Tuleya, 1974).

Notice that the total energy consists mostly of total potential energy (95.8%). Even at the mature stage of hurricane development, less than 0.1% of the total energy is kinetic energy and only 4.2% is latent energy. For the 498 km domain, the flux terms are small for the mean and eddy kinetic energy, but very large in the budgets of total potential and latent energy. This indicates that the kinetic energy is more or less self-contained within a 500 km area. Starting with the eddy kinetic energy, the budgets for each of the four energy boxes in Fig. 2 will be discussed separately.

The eddy kinetic energy K_E is primarily due to the asymmetric motion within 200 km radius at upper levels (Kurihara and Tuleya, 1974, Fig. 10). As Fig. 2 shows, eddy kinetic energy is exported from the subdomain of 498 km radius, but the contribution of this outgoing flux to the total energy budget is small.

At smaller radii the transport is important in the local budget of eddy kinetic energy. Fig. 3 shows the distribution of the eddy kinetic energy budget terms with radius for the same time period. Most of the contributing quantities to the budget are confined to the inner 100 km of the storm. For this region conversion of mean kinetic and total potential energy are the source of K_E and are nearly equal in magnitude. They are balanced by both frictional dissipation and strong export caused by mean and eddy flow. Both sink terms are large in the upper atmosphere where eddies predominate.

This result conflicts with Anthes' (1972) analysis of the eddy kinetic energy. In his model tropical cyclone study, conversion from potential energy was not a significant source of eddy kinetic energy. Indeed, in the upper two levels of his model experiment, eddy kinetic energy was converted into potential energy. The conversion of mean kinetic energy to eddy kinetic energy in the inner 498 km region of the GFDL model was approximately 5×10^{12} W during the mature stage. Although this is comparable to Anthes' result (integral for 440 km domain is $\sim4\times10^{12}$ W), eddy kinetic energy in his model was converted to total potential at a rate less than 1×10^{12} W. In the GFDL model, total potential energy was converted to eddy kinetic energy at a rate of $\sim4\times10^{12}$ W.

Riehl and Malkus (1961) made estimates of eddy transports of kinetic energy, $\{\mathrm{FLXE}\}_E$ in the present notation, on two days of hurricane Daisy. Unfortunately, only a few flight levels of data are available which makes comparison with the model hurricane somewhat awkward. At any rate, the GFDL model seems to agree more with their second day's results when eddy kinetic energy transports were quite large and directed outward from the storm center. Divergence of eddy kinetic energy due to this outward transport in Daisy is estimated to be approximately 25×10^{-4} erg cm^{-2} s^{-1} at 55 km radius. This is comparable to the flux divergence of K_E at this radius in the model, i.e., 23×10^{-4} erg cm^{-2} s^{-1}.

The eddy kinetic energy beyond 130 km radius is maintained by transport from the inner area. Contribution of energy conversions from mean kinetic or total potential to the budget of eddy kinetic energy in this outer area is negligible. This agrees with the analysis result of spiral bands by Kurihara and Tuleya (1974); namely, once the band is formed in an area surrounding

the center, it propagates outward apparently without any further appreciable supply of energy.

It is interesting to look at the storm during a period of early development. Fig. 4 is the same as Fig. 3 except for Hours 40–49 and a change of scale. At this time both the eddy and mean kinetic energy were increasing. Compared to Fig. 3 $\{TP,K_E\}$ dominates over $\{K_M,K_E\}$ in the early development stage. As expected from the larger dimension of the vortex in this stage, the budget quantities are not as confined to the center, but exhibit a broad distribution.

Based on the above results, one may guess that the eddies develop through $\{TP,K_E\}$ at first but receive additional energy from $\{K_M,K_E\}$ at the mature stage of the storm. On the other hand, a different speculation is possible about the evolution of eddies. There may exist two distinct kinds of eddies, each being energetically more or less independent of the other, and the one related to the inertial instability of the mean flow may develop later than the eddies originating from eddy conversion of potential energy. Further study is needed to clarify this matter.

c. Mean kinetic energy budget

The radial distribution of the mean kinetic energy budget is given in Fig. 5 for the mature storm period. In general, the budget terms are at least more than twice as large as the analogous terms in the eddy kinetic energy budget even in the storm's core where the eddies are most significant. Nevertheless, the conversion term $\{K_M,K_E\}$ is by no means negligible compared to the other terms in the mean kinetic energy budget. The model's result agrees with those of Palmén and Riehl (1957) and Ooyama (1969) that production is smaller than dissipation in the interior and that advection of mean kinetic energy from outer radii maintains the balance of mean kinetic energy. Note that for the entire region, 0–498 km radius, production is balanced by frictional dissipation and eddy conversion (Fig. 2). As seen in Fig. 5, production contributes more than advection as a local energy source for the area inside 150 km. This is in agreement with the analyses by Riehl and Malkus (1961) and Palmén and Riehl (1957). The findings of Hawkins and Rubsam (1968) indicate the contribution of advection within a 150 km radius was larger than that of production.

The mean surface dissipation and mean internal dissipation were also computed for the model. It was found that the mean surface dissipation accounts for 20% of the mean total dissipation near the center, 55% at 100 km, and approximately 80% from 200 to 500 km. In general, this result coincides with that of Riehl and Malkus (1961) obtained for an inner area of hurricane Daisy. Hawkins and Rubsam's analysis showed an increase of relative importance of surface friction with decreasing radius, although they mentioned that internal dissipation may be more significant than their results indicated.

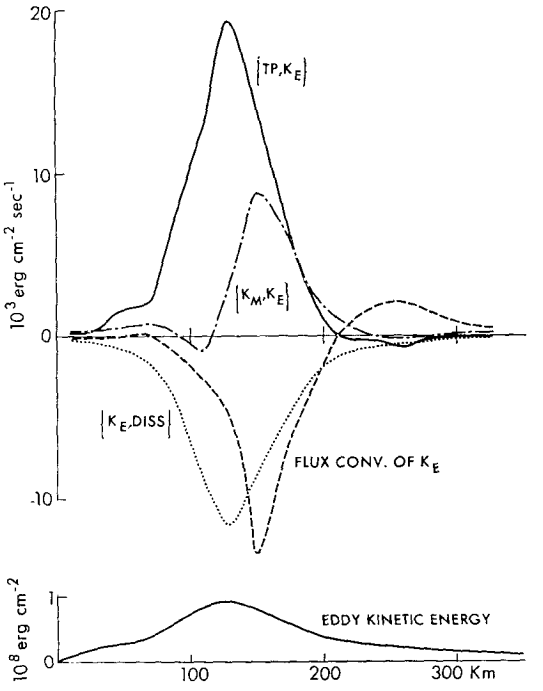

FIG. 4. Radial distribution of eddy kinetic energy and eddy kinetic energy budget for early development period (Hours 40–49). Values are vertically integrated, area averages. Similar to Fig. 2 except for change of scale.

One can compare the results of the total kinetic energy budget of the present analyses to those obtained by Anthes (1972). The conversion of total potential energy for the 440 km region was estimated to be 36×10^{12} W in Anthes' analysis which compares with the 32×10^{12} W calculated during Hours 150–159 for the 498 km region in the GFDL model. The dissipation of total kinetic energy according to Anthes was estimated at 35×10^{12} W compared to 29×10^{12} W for a comparable period in the GFDL model. In the present analysis, the difference between conversion and dissipation results, in part, from an export of kinetic energy from the 498 km region by eddy motion.

d. Total potential energy

The radial distribution of the budget terms of total potential energy for the mature storm is given in Fig. 6. Export of potential energy, which takes place mostly in the upper levels, is balanced by pressure work, heating due to latent heat release, and import of internal energy in the lower layers.

The export of potential energy, i.e., $\langle\bar{v}_r\bar{\phi}\rangle$ larger than zero, at the mature stage is consistent with maintaining both a warm core and a high level of kinetic energy in the storm. Strong low-level inflow and upper-level outflow which establishes a large export of potential energy

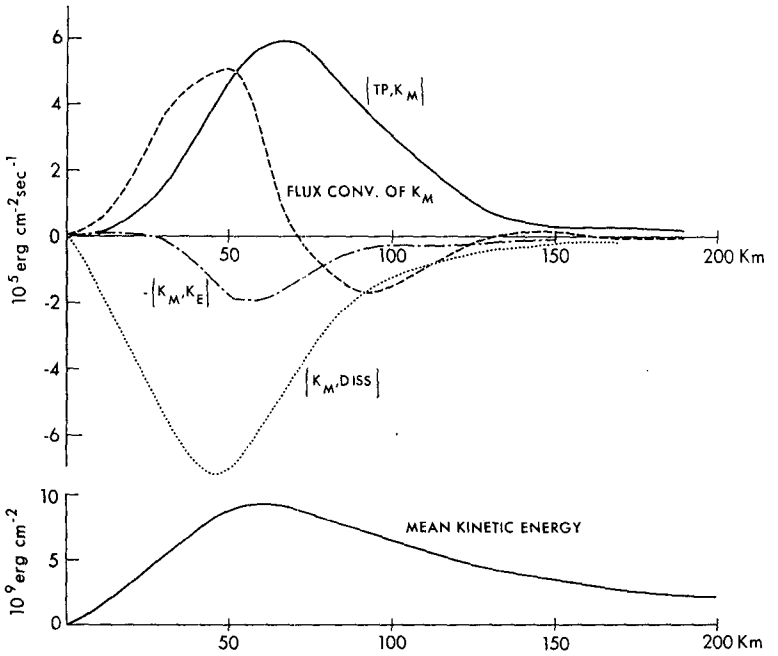

FIG. 5. Radial distribution of mean kinetic energy and mean kinetic energy budget for mature storm period (Hours 150–159). Values are vertically integrated, area averages. Changes due to flux convergence (dashed line), conversion from K_E (dash-dotted line), conversion from TP (thick solid line), and dissipation (dotted line) are shown.

is, of course, associated with strong upward motion in the core region. On the one hand, the low-level convergence of moisture and the upward motion bring about the release of latent heat. This compensates for the adiabatic cooling, and the baroclinicity field responsible for the radial vertical circulation is therefore maintained. On the other hand, such a circulation in the presence of a warm core generates kinetic energy, i.e.,

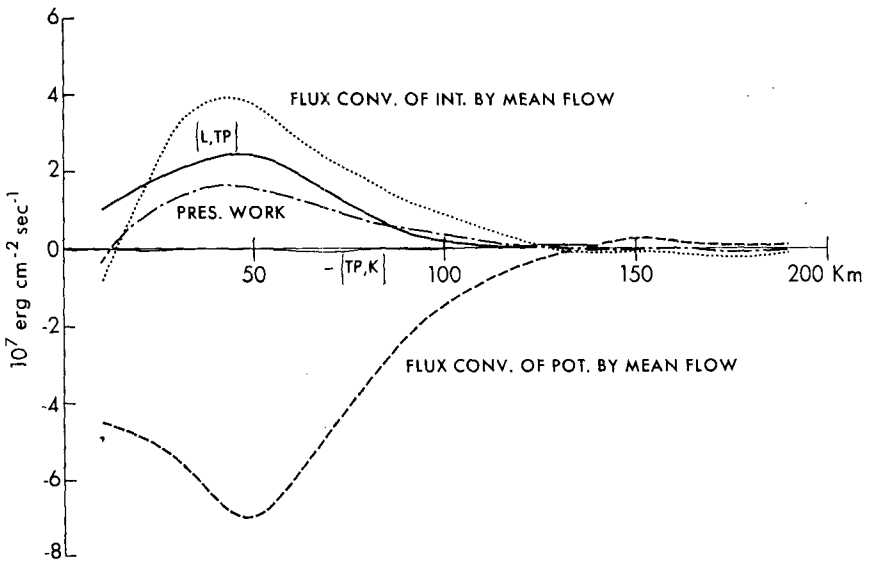

FIG. 6. Radial distribution of total potential energy budget for mature storm period (Hours 150–159). Values are vertically integrated, area averages. Changes due to flux convergence of internal energy by mean flow (dotted line), conversion from LR (thick solid line), pressure work (dash-dotted line), conversion to K_M and K_E (thin solid line), and flux convergence of potential energy (dashed line) are shown. Other quantities are too small to be plotted.

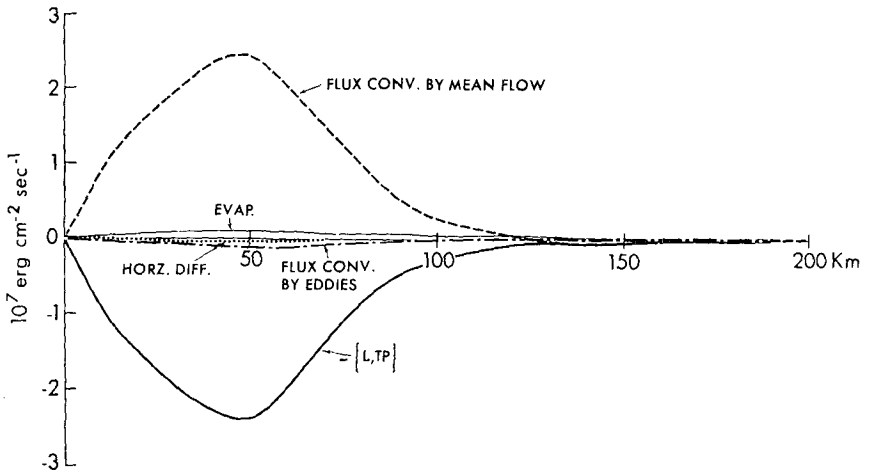

FIG. 7. Radial distribution of latent energy budget for mature storm period (Hours 150–159). Values are vertically integrated, area averaged. Changes due to flux convergence by mean flow (dashed line), flux convergence by eddies (dash-dotted line), conversion to *TP* (thick solid line), evaporation (thin solid line), and horizontal diffusion (dotted line) are shown.

$\langle -\bar{v}_r \nabla \bar{\phi} \rangle$ larger than zero, as was pointed out by Palmén and Riehl (1957).

Fig. 6 shows that the loss of total potential energy through generation of kinetic energy is almost negligible compared to the other terms of the potential energy budget. The contributions from the field asymmetries and the diffusion terms, including the surface heat flux, are so small that they cannot be plotted. The heat engine efficiency of the storm as defined by the expression $(TP,K)/(L,TP)$, for the 498 km area is approximately 6%. The heating rate of the model described by Anthes (1972) was given as 12.6×10^{14} W. This figure is higher than the present model's result which for the 498 km region is 5.7×10^{14} W. Of course, the heating rate is quite variable depending on the size, intensity and stage of development of a hurricane. For the mean tropical cyclone analysis of Palmén and Riehl (1957) the heating rate was estimated at 5.54×10^{14} W for a domain between the radial intervals of 28 and 222 km. For the domain area within a radius of 148 km, Riehl and Malkus (1961) estimated the heating rates of Daisy to vary from 1.91×10^{14} W on 25 August to 4.40×10^{14} W on 27 August 1958.

e. Latent energy

Fig. 7 displays the latent energy budget distribution for the mature storm. In general, the loss of moisture due to heavy precipitation in the storm's interior is compensated by the inflow of latent energy by the mean flow from the outer periphery of the storm. The role of evaporation in the budget of latent energy in the interior appears to be small but is believed to be important because of its effect of increasing the equivalent potential temperature of inflowing, low-level air. Without this effect the very warm storm core, the low surface pressure at the center, and the intense hurricane force winds would not be possible.

The eddies export latent energy in the model. Riehl and Malkus (1961) computed the eddy transport of moisture for hurricane Daisy. However, a reliable determination could not be made because of the uncertainty of the data. Eddy export in the model is largest at mid-levels in the interior region about 70 km from the center. However, as suggested from Fig. 7, the net transport of latent energy is largely due to the mean flow and is directed inward.

f. Fluxes of energy

In this subsection the radial fluxes of energy by the eddies and by the mean flow are summarized. The computed fluxes indicate the energy amounts which flow across each radius circle per unit time. The average is taken for Hours 150 through 159. Fig. 8 displays the eddy fluxes of kinetic, internal and latent energy, and the pressure work relating to the eddy motion. All eddy fluxes are large only in the inner 250 km. For almost the entire 500 km region, the eddies export energy from the storm's center. This is opposite to the transport by the mean flow to be shown later.

The eddy transports of meteorological variables are related to the structure of eddies or waves. In the present model, the spiral bands appear to be one of the components of asymmetry. The eddy fluxes of some quantities evaluated in the present analysis may be explained in terms of the band structure.

According to the analysis by Kurihara and Tuleya (1974), the spiral band is a convergence zone at low and high levels and a divergence zone at middle levels. The convergence or divergence is caused by a variation in inflow angle of the horizontal wind between the

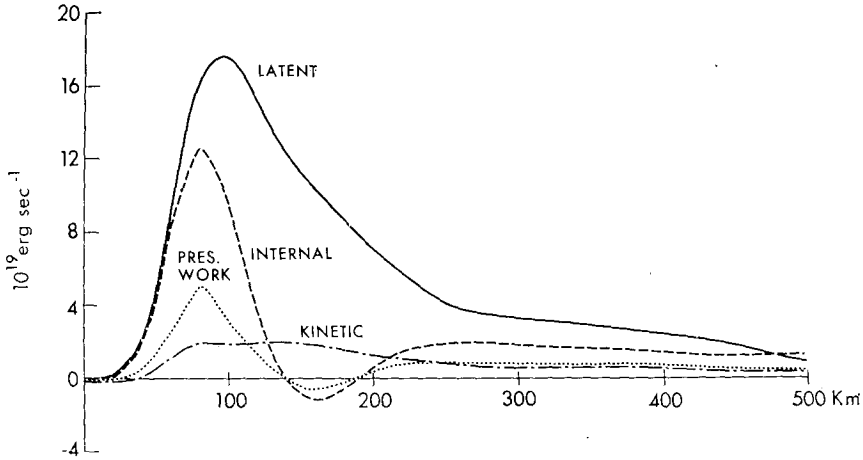

FIG. 8. Radial distribution of flux of energy by eddies for mature storm period (Hours 150–159). Values are vertically integrated. Positive values denote outward transport.

leading and rear edge of the band. Along the leading edge there exists a low pressure system at low and high levels and a high pressure system at middle levels. A typical orientation of spiral bands developed in the model is shown in Fig. 1. Based on these results, a schematic figure showing the distribution of pressure and horizontal wind vectors at low levels near the band is shown in Fig. 9. At point A in the figure the quantities v_θ', v_r' and p' are all negative, while they are positive at point B. Therefore, both $\overline{v_\theta' v_r'}$ and $\overline{p' v_r'}$ are presumably positive. The same results can be obtained for the upper and middle levels. Consequently, the outward eddy flux of pressure work and, hence, that of internal energy are consistent with the structure of spiral bands. It will be shown later that eddies also export angular momentum from the storm center which is consistent with $\overline{v_\theta' v_r'}$ being positive in spiral bands.

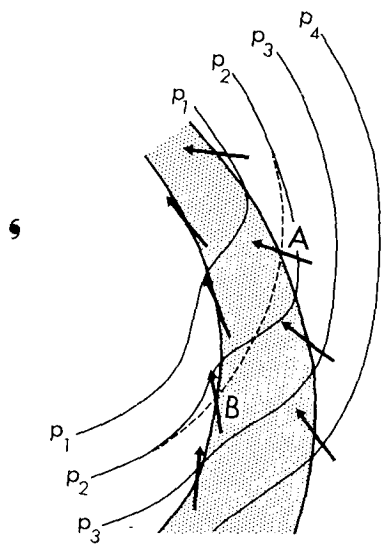

FIG. 9. Schematic figure showing the distribution of surface wind (arrows) and pressure (solid lines, $p_1 < p_2 < p_3 < p_4$) in the vicinity of a spiral band, typical of those developed in the model. The spiral band area is shaded. Points A and B lie on the same radius circle which is denoted by a dashed line.

The relationships among the transports, both horizontal and vertical, of various quantities by waves may be explained by the phase speed and tilt of the waves, the distribution of basic flow, the static stability of the basic state, and other factors. This seems to be an interesting subject to be studied in the future.

In the model, eddy transports of only the kinetic energy and to some degree the latent energy are significant compared to their respective mean transports. All other eddy transports are less than 5% of the mean transports. The export of energy by eddies conflicts with the analysis of Hawkins and Rubsam (1968), but agrees with some estimates made by Riehl and Malkus (1961). Caution should be used in interpreting the results, however, because of the physical restraints of the model cyclone and the somewhat unrealistic flow in the upper layers of the model (Kurihara and Tuleya, 1974).

The fluxes of energy and pressure work by the mean flow are shown in Fig. 10. Energy is transported inward largely in the form of internal and latent energy as well as pressure work. Compensating outflow of energy takes place in the form of potential energy transport. The flow of kinetic energy is two orders of magnitude smaller than the other mean fluxes.

The mean fluxes are not small at the outer radii because the larger circumference compensates for the smaller magnitude per unit circumference. The energy fluxes by the mean flow vary sharply within about 120 km of the center. Therefore, as discussed earlier in the budget analysis of each form of energy, the convergence or divergence of energy in any form is considerably large in the small central area.

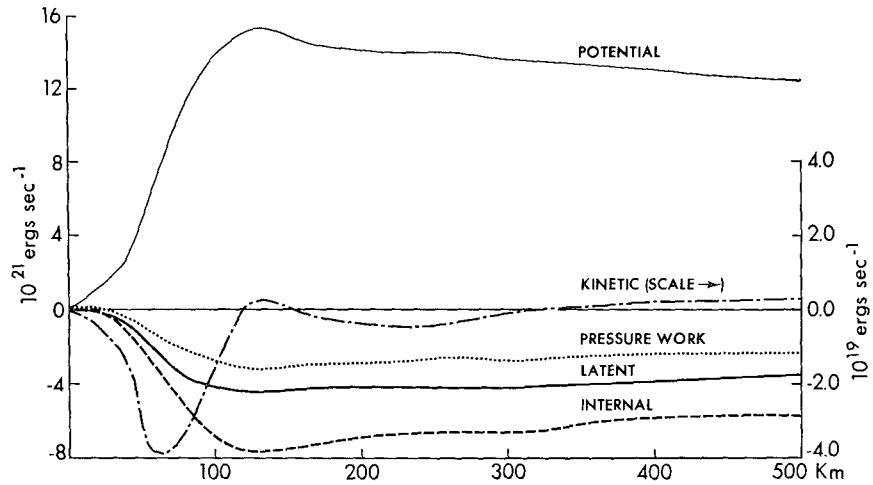

FIG. 10. Flux of energy by mean flow versus radius for mature storm period (Hours 150–159). Values are vertically integrated. Positive values denote outward transport.

4. Angular momentum

a. Equation for relative angular momentum

The equation for relative angular momentum RAM can be obtained from the equation for the tangential component of velocity [(2.2)] by multiplying by r, separating the basic quantities into mean and eddy parts, and then averaging the equation along the azimuthal direction. The vertical integral of the resulting equation yields

$$\begin{aligned}
&\frac{\partial}{\partial t}\langle p_* r\bar{v}_\theta\rangle = && \text{tendency of relative angular momentum}\\
&-\frac{1}{r}\frac{\partial}{\partial r}(r\langle p_* r\bar{v}_r\bar{v}_\theta\rangle) && \text{mean flux convergence of RAM}\\
&-\frac{1}{r}\frac{\partial}{\partial r}(r\langle p_* r\overline{v_r'v_\theta'}\rangle) && \text{eddy flux convergence of RAM}\\
&-fr\langle p_*\bar{v}_r\rangle && \text{Coriolis turning}\\
&+r\langle {}_H F_\theta\rangle && \text{horizontal diffusion}\\
&+r\langle {}_v F_\theta\rangle && \text{vertical diffusion of RAM}
\end{aligned} \qquad (4.1)$$

where the angle brackets and all other quantities used in (4.1) were described in Section 3a. The Coriolis turning denotes the tangential torque acting on the radial flow. Using the continuity equation, this term can be rewritten as

$$-fr\langle p_*\bar{v}_r\rangle = -\frac{\partial}{\partial t}\left\langle p_*\frac{f}{2}r^2\right\rangle - \frac{1}{r}\frac{\partial}{\partial r}\left(r\left\langle p_*\frac{f}{2}r^2\bar{v}_r\right\rangle\right). \qquad (4.2)$$

Thus, the equation for absolute angular momentum, $rv_\theta + (f/2)r^2$, is quite similar to (4.1) except that the Coriolis term is replaced by the flux convergence of earth angular momentum.

b. Relative angular momentum budget

The budget of RAM was computed for a 498 km radius area using (4.1) and time-averaged for the same period as the energy budget (Hours 150–159). For the 498 km area the balance is mostly between the mean flux convergence of RAM and the loss of RAM through surface friction. Fig. 11 is a box diagram of the results. Both Coriolis and eddy effects are small compared to the other budget terms for the 498 km area.

The radial distribution of the RAM budget for the mature storm period is shown in Fig. 12. In the interior 150 km, the eddy flux divergence is quite large, ~30%

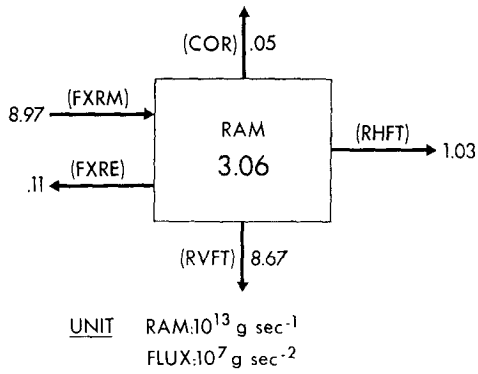

FIG. 11. Relative angular momentum budget for inner 498 km of the model hurricane, averaged for Hours 150–159. The area averages of flux convergences and conversions are in units of 10^7 g s^{-2}. The area average of relative angular momentum, RAM, given within the box, is in units of 10^{13} g s^{-1}. FXRM: mean flux convergence of RAM; FXRE: eddy flux convergence of RAM; COR: coriolis turning; RHFT: horizontal diffusive flux convergence of RAM; RVFT: vertical diffusive flux convergence of RAM through surface stress.

of the mean convergence. As in the case of the energy budget, the eddies export angular momentum from the storm's center. The possible role of spiral bands in this eddy export was discussed in Section 3f. Horizontal diffusion is also quite large near the storm's center which indicates that small-scale lateral stress is significant in the budget of RAM.

The RAM is lost through surface friction at all radii throughout the whole integration period. Therefore, the total angular momentum of the system keeps decreasing with time. A steady field of RAM has not been attained by the end of the present integration, although a quasi-stationary state is evident for the storm area within a few hundred kilometers during the mature stage.

The radial distribution of the vertically integrated relative angular momentum is shown for various times during the model cyclone's history in Fig. 13. Notice the negative values of the vertical integral of RAM beyond 700 km, which reflects the development of anticyclonic flow in the upper outer region. During the development of the storm, the inward flux of RAM by the mean flow was large which contributed to the increase of RAM in the inner area. The loss of RAM at the surface as compared to the loss at the mature stage was also smaller.

c. Comparison with observations and other models

For the mature stage, the absolute angular momentum budget was computed by dividing the model hurricane into two composite layers of nearly equal mass—the upper five model levels and the lower six model levels. Fig. 14 shows the transport across the boundary of each subdomain in the 500 km region. The transport by eddies is comparable to the mean flow transport only in the upper levels and for the interior 200 km. Notice that almost all eddy transports and all small-scale lateral stresses are directed outward. Palmén and Riehl (1957) found from observational

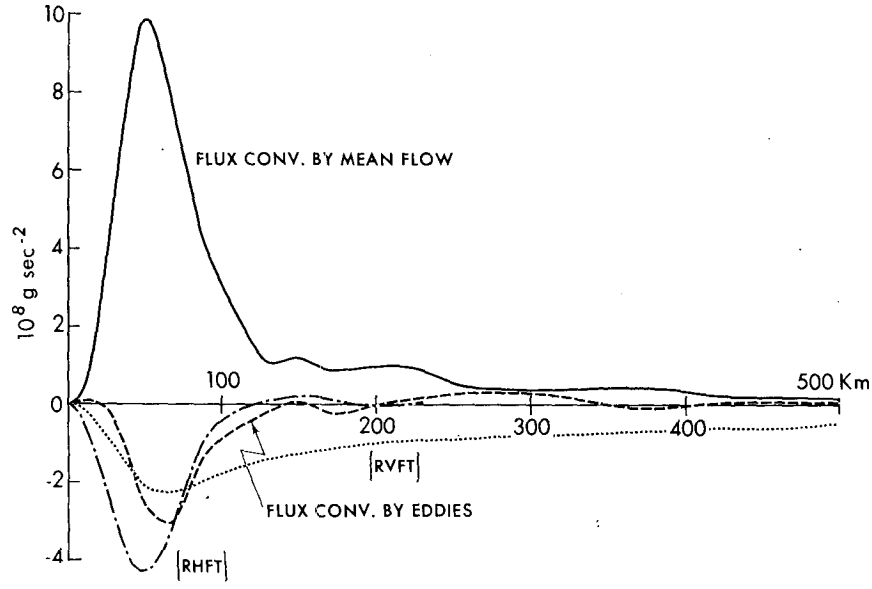

FIG. 12. Radial distribution of the relative angular momentum budget for the mature storm period (Hours 150–159). Values are vertically integrated, area averages. Changes due to the flux convergence of RAM by the mean flow (thick solid line), flux convergence of RAM by eddies (dashed line), vertical diffusive flux convergence {RVFT} (dotted line), and horizontal diffusive flux convergence {RHFT} (dash-dotted line) are shown. Coriolis turning is too small to be graphed.

analysis that the eddy transport was directed inward, although their estimates of eddy contributions are due entirely to a mean asymmetric basic flow superposed on a circular symmetric hurricane vortex. For the mean flow Palmén and Riehl's data had the same sign, but the magnitude is generally larger than the model's results. Black and Anthes (1971) computed the eddy and mean transport of RAM at the outflow level for individual storms as well as for a mean hurricane and a mean typhoon. Their result shows an inward transport by eddies. This is in agreement with the estimate of Palmén and Riehl, and in contrast to the result from the present model.

Fig. 15 shows the distribution of flux of absolute angular momentum by the mean flow, eddies and diffusion, respectively, for the model hurricane and corresponding observational analyses for the inner region of the storm. In general, the model agrees with the second day of Daisy (Riehl and Malkus, 1961). However, the model imports significantly larger amounts of angular momentum by low-level mean flow than indicated by Hawkins and Rubsam's analysis and the first day of Daisy. As mentioned before, the model eddies export angular momentum and are just as important as the mean flow in exporting angular momentum in the interior 200 km in the upper atmosphere. As mentioned by Riehl and Malkus (1961), the lateral diffusion of angular momentum is not insignificant in the storm's core.

The momentum losses to the sea per unit area were calculated and compared to the values estimated from Palmén and Riehl's (1957), Hawkins and Rubsam's (1968), and Riehl and Malkus' (1961) data. The results are shown in Fig. 16. Note that the arm length is multiplied by the surface stress to obtain the values so that the stress maximum is located inside the peak of angular momentum loss. The model's result is larger than those for Daisy and Hilda, but smaller than Palmén and Riehl's estimates. The differences of the results may be caused by the natural variability of hurricanes as well as by analysis methods.

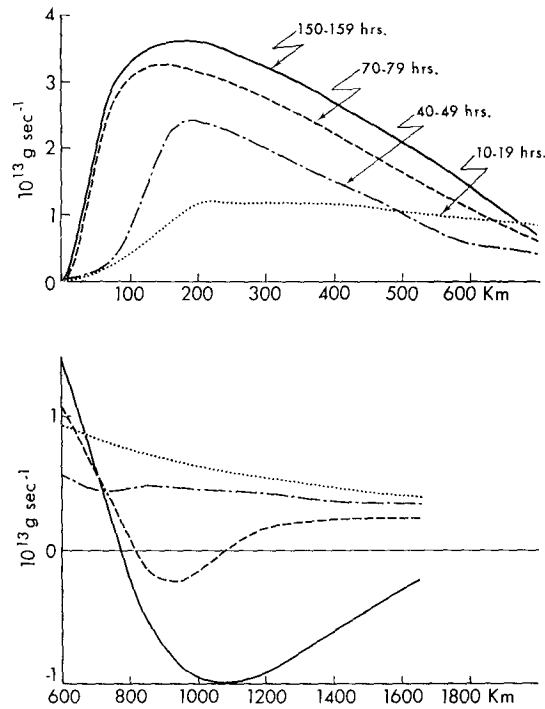

FIG. 13. Radial distribution of vertically integrated relative angular momentum for four different time periods of the storm's evolution.

Next, the transport of RAM in the present model is compared with those in other three-dimensional nu-

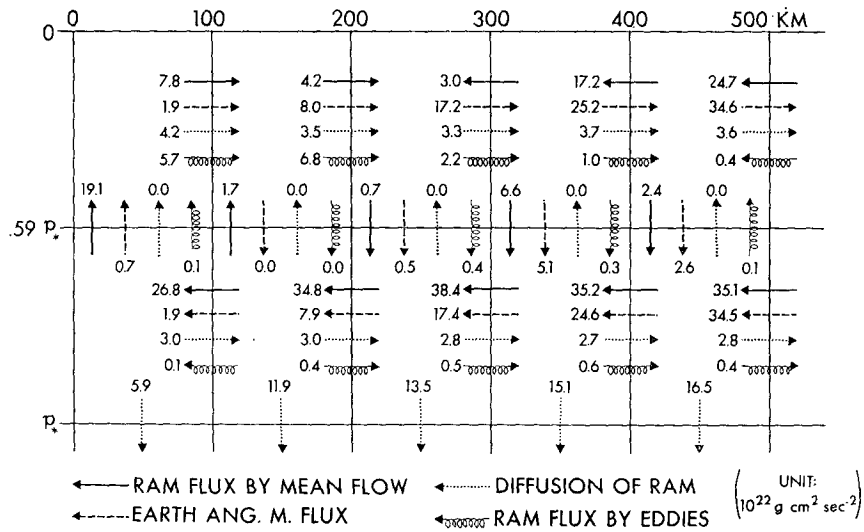

FIG. 14. Transport of angular momentum from one 100 km subdomain to another by various transport processes. Vertical division is at $p/p_* \approx 0.59$. Units are in 10^{22} gm cm^2 s^{-2}.

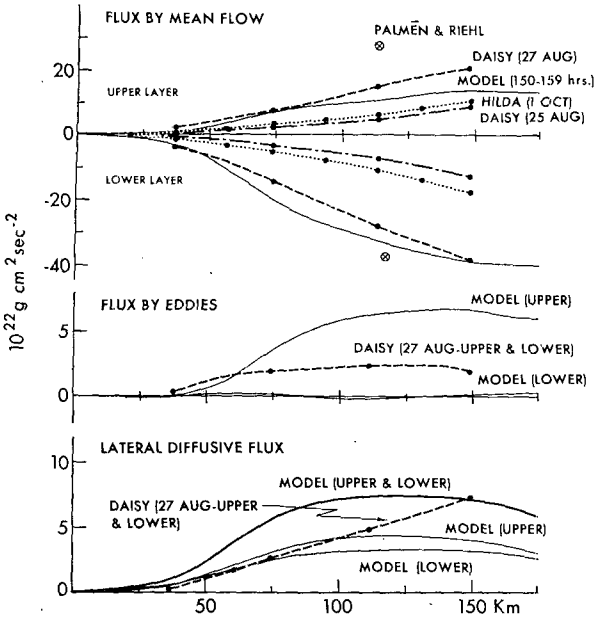

FIG. 15. Flux of angular momentum by mean, eddy and lateral diffusive flow for inner storm region. Comparison made with real data analysis of Daisy (Riehl and Malkus, 1961), Hilda (Hawkins and Rubsam, 1968), and a mean tropical cyclone (Palmén and Riehl, 1957).

merical models. Trout and Anthes (1971) made analysis of asymmetries within a radius of 350 km in the model constructed by Anthes *et al.* (1971). Note that neither the present model nor their model contains an asymmetric basic current. The eddy transport of relative angular momentum is directed outward in the outflow layer in both models. The value of $\overline{v_\theta' v_r'}$ at 300 km radius is 2.8 m^2 s^{-2} at level 1 (225 mb) in their model and 0.65 m^2 s^{-2} averaged for the top half of the atmosphere in the present model. The transport by the mean flow in the outflow layer is outward in the inner region but inward beyond 135 km radius in their model and beyond about 250 km radius in the present model. This reflects the difference in the radii where the azimuthal wind changes from cyclonic to anticyclonic flow at the outflow level in each model. In the lower layers, the eddy transport is negligibly small and the large flux by the mean flow is toward the center in both models. The contribution of eddies to the vertical transport in Trout and Anthes' analysis is very small at all radii and that of the mean motion is large and upward within 100 km radius. This result is the same with the one obtained from the present model. Mathur (1972) integrated a three-dimensional hurricane model starting from observed initial data. At the hurricane stage, the vertically integrated value of the horizontal eddy transport shows an outward flux of relative angular momentum at 3°, 4° and 6° latitude radii. The direction of total flux is inward. The value of $\overline{v_\theta' v_r'}$ is very large in his case not only at the outflow level but also at the inflow level. Its value at 300 mb at 3° latitude radius is computed as 65.7 m^2 s^{-2}.

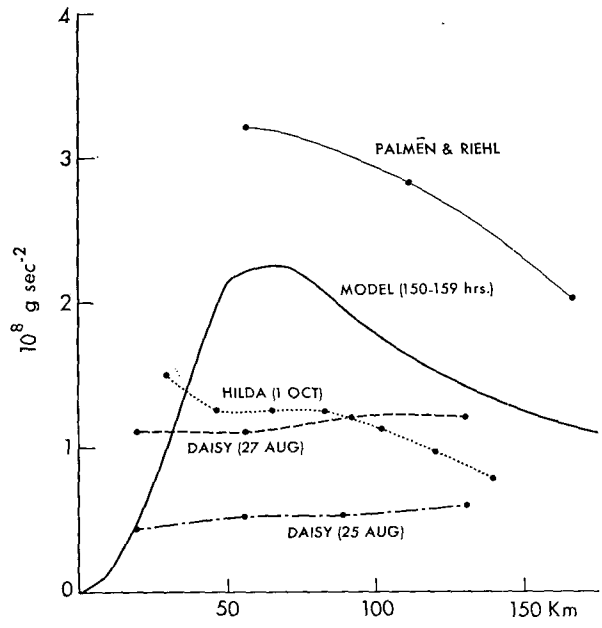

FIG. 16. Angular momentum losses to the sea per unit area for inner storm region. Comparison made with real data analyses of Daisy (Riehl and Malkus, 1961), Hilda (Hawkins and Rubsam, 1968), and a mean tropical cyclone (Palmén and Riehl, 1957).

5. Summary

From the present budget analyses, the following features of the three-dimensional hurricane simulated with the GFDL numerical model are evident:

The eddy kinetic energy of the model is supported at the mature stage by supply from both mean kinetic and total potential energy. Conversion of energy from total potential energy seems more important for the evolution of asymmetries in the early stages of hurricane development, as far as the present model hurricane is concerned.

The eddies developed in the present model export latent, internal and kinetic energy, as well as relative angular momentum from the inner area of the storm. The pressure work associated with eddy motion also transfers energy from the inner area to the outer region. This is opposite to the dominant inward transport of these quantities by the mean flow.

Although the eddies' contribution to the budgets of kinetic and latent energy and of angular momentum in the inner region is not negligibly small, the energy and relative angular momentum budgets of the present model are primarily determined by the mean flow. It imports latent, internal and kinetic energy into the inner area and yields a large outward flux of potential energy. These main features agree with the results of observational analyses and other model experiments.

The dominant role of the mean flow in hurricane dynamics was pointed out by Riehl and Malkus (1961). This is probably one of the factors which contributed to the qualitatively successful simulation of tropical cyclones by axisymmetric models.

Finally, it should be noted that the results of the analyses concerning the role of eddies in the present model conflict with some of the observational analyses while agreeing with others. The recognition of eddies in real hurricanes may be partly due to the asymmetry of a basic field on which a hurricane is superposed. On the other hand, the eddies in the present model are the distorted features of an initially circular vortex isolated in a closed domain and do not involve any wind component associated with a basic flow. A further analysis of the numerical results from a model without such a restraint is needed.

Acknowledgments. The authors are indebted to Dr. J. Smagorinsky who has given them many valuable suggestions and support throughout the course of the tropical cyclone project. We are also grateful to Drs. R. Gall, Y. Hayashi and A. H. Oort who read the original manuscript and gave useful, constructive criticism. Finally, it is a pleasure to express gratitude to Messrs. J. N. Conner and P. G. Tunison and Mrs. E. J. D'Amico for their assistance in the preparation of this manuscript.

REFERENCES

Anthes, R. A., 1972: Development of asymmetries in a three-dimensional numerical model of the tropical cyclone. *Mon. Wea. Rev.*, **100**, 461–476.

——, S. L. Rosenthal and J. W. Trout, 1971: Preliminary results from an asymmetric model of the tropical cyclone. *Mon. Wea. Rev.*, **99**, 744–758.

Black, P. G., and R. A. Anthes, 1971: On the asymmetric structure of the tropical cyclone outflow layer. *J. Atmos. Sci.*, **28**, 1348–1366.

Hawkins, H. F., and D. T. Rubsam, 1968: Hurricane Hilda, 1964: Structure and budgets of the hurricane on October 1, 1964. *Mon. Wea. Rev.*, **96**, 617–636.

Kurihara, Y., 1975: Budget analysis of a tropical cyclone simulated in an axisymmetric numerical model. *J. Atmos. Sci.*, **32**, 25–59.

——, and R. E. Tuleya, 1974: Structure of a tropical cyclone developed in a three-dimensional numerical simulation model. *J. Atmos. Sci.* **31**, 893–919.

Malkus, J. S., and H. Riehl, 1960: On the dynamics and energy transformations in steady-state hurricanes. *Tellus*, **12**, 1–20.

Mathur, M. B., 1972: Simulation of an asymmetric hurricane with a fine mesh multiple grid primitive equation model. Rept. No. 72-1, Dept. of Meteorology, Florida State University.

Ooyama, K., 1969: Numerical simulation of the life cycle of tropical cyclones. *J. Atmos. Sci.*, **26**, 3–40.

Palmén, E., and H. Riehl, 1957: Budget of angular momentum and energy in tropical cyclones. *J. Meteor.*, **14**, 150–159.

Phillips, N. A., 1957: A coordinate system having some special advantages for numerical forecasting. *J. Meteor.*, **14**, 184–185.

Riehl, H., and J. S. Malkus, 1961: Some aspects of hurricane Daisy, 1958. *Tellus*, **13**, 181–213.

Trout, J. A., and R. A. Anthes, 1971: Horizontal asymmetries in a numerical model of a hurricane. NOAA Tech. Memo. ERL NHRL-93, National Hurricane Research Laboratory, Coral Gables, Fla., 37 pp.